Electronic Supplementary Material (ESI) for Chemical Science.

Identification of key structural features of the elusive Cu-Aβ complex generating ROS in Alzheimer's Disease

Clémence Cheignon, Megan Jones, Elena Atrián-Blasco, Isabelle Kieffer, Peter Faller, Fabrice Collin and Christelle Hureau

Supporting Information

Experimental section

EPR measurements

EPR spectra were recorded on a Bruker Elexsys E500 spectrometer equipped with a continuous flow cryostat (Oxford). Analysis was performed with aqueous solution containing 10% of glycerol, ^{65}Cu (450 µM) and peptide (500 µM, $A\beta_7$, H6A-H13A-$A\beta_{16}$, H6A-H14A-$A\beta_{16}$, D7H-$A\beta_{16}$, D1E-$A\beta_{16}$, D1N-$A\beta_{16}$ or $A\beta_{16}$). pH was adjusted with H_2SO_4 (1 M) and NaOH (1 M). Experimental parameters were set as following: T = 120 K, ν = 9.5 GHz, microwave power = 20.5 mW, Amplitude modulation = 5.0 G, Modulation frequency = 100 kHz.

Cu K-edge X-ray Absorption Data Collection and Measurement

The copper-containing Aβ solutions were injected into sample holders in between two windows made of Kapton tape (3M, cat. #1205; Minneapolis, MN) and quickly frozen in liquid nitrogen. All samples were maintained at 10-20 K throughout the data collection using a helium cryostat. Cu K-edge XANES (X-ray absorption near edge structure) spectra were recorded at the BM30B (FAME) beamline of the European Synchrotron Radiation Facility (ESRF, Grenoble, France)[1]. The storage ring was operating in 7/8+1 multibunch filling mode at 6 GeV with a ~ 200 mA current. The beam energy was selected using an Si(220) N_2 cryo-cooled double-crystal monochromator with an experimental resolution close to that theoretically predicted (namely ~ 0.5 eV)[2]. The beam spot on the sample was approximately 300 x 100 μm^2 (H x V, FWHM). The spectra are reported as fluorescence data, which were recorded utilizing a 30-element Ge solid-state fluorescence detector (Canberra). The energy was calibrated with a Cu metallic foil, such that the maximum of the first derivative was set at 8979 eV. Cu data were collected differently in 3 regions: from 8830 to 8960 eV using 5 eV steps and counting 2 s per point, from 8960 to 9020 eV using 0.5 eV steps and counting 3 s per point, and from 9020 to 9300 eV with a k-step of 0.05 $Å^{-1}$ and an increasing counting time of 2 to 10 s per point.

For each sample, three scans were averaged and XANES spectra were background-corrected by a linear regression through the pre-edge region and a polynomial through the post-edge region and normalized to the edge jump. This data treatment was carried out using the software Athena. The beam was moved to a different position on the sample for each scan to avoid potential Cu photoreduction. All spectra were individually inspected prior to data averaging to ensure that sample decomposition in the beam was not occurring.

Cu(I) samples were prepared by direct addition (10 equiv.) of fresh made $Na_2S_2O_4$ stock solution (0.1M) and Cu(II) 10 mM into the sample holder containing the peptide in the presence of 10% glycerol as cryoprotectant and under a continuous flow of N_2. The sample was immediately frozen in liquid nitrogen. In such conditions, no significant pH drift due to the addition of $Na_2S_2O_4$ was measured.

High-Resolution Mass spectrometry

High resolution mass spectrometry (HPLC/HRMS) analysis was performed on a LTQ-Orbitrap XL mass spectrometer (ThermoFisher Scientific, Les Ulis, France) equipped with an electrospray ionization source and coupled to an Ultimate 3000 LC System (Dionex, Voisins-le-Bretonneux, France). The Orbitrap cell was operated in the full-scan mode at a resolution power of 60 000. Sample (10 µL) was injected into the column (Phenomenex, Kinetex RP-C18, 50 × 3 mm, 2.6 µm), whose temperature was maintained at 25°C. Gradient elution was carried out with formic acid 0.1% (mobile phase A) and acetonitrile/water (80/20 v/v) formic acid 0.1% (mobile phase B) at a flow-rate of 500 µL min-1. The mobile phase gradient was programmed with the following time course: 5% mobile phase B at 0 min, held 3 minutes, linear increase to 45% B at 8 min then to 100% B at 9 min, held 2 min, linear decrease to 5% B at 12 min and held 3 min. The mass spectrometer was used as a detector, working in the full scan positive mode between 150 and 1200 Da. Trace chromatograms of Aβ and oxidized species were obtained in QualBrowser software (ThermoScientific), at 6 ppm mass accuracy.

^{1}H NMR spectroscopy

Studies were performed or D_2O. However, for clarity and consistency, we decided to use the notation pH even when the measurements were made in D_2O. The pD was measured using a classical glass electrode according to pD = pH* + 0.4, and the apparent pH value was adjusted according equation pH = (pD − 0.32)/1.044,[3] or equivalently according equation pH = 0.929pH* + 0.41,[4] to be in ionization conditions equivalent to those in H_2O.

Stock solutions of $A\beta_7$ and H6A-H13A were prepared by dissolving the powder in D_2O. H6A-H13A concentration was then determined by UV-visible absorption of tyrosine Tyr10 considered as free tyrosine (ε(276)-ε(296) = 1410 $M^{-1}cm^{-1}$) and $A\beta_7$ concentration was determined by UV-visible absorption of phenylalanine Phe4 considered as free phenylalanine (ε(258)-ε(280) = 195 $M^{-1}cm^{-1}$).

Cu(I) addition to $A\beta_7$ or H6A-H13A was carried out as follow: 1 equivalent of Cu(II) was added to a 0.5 mM solution of peptide in 0.2 M phosphate buffer in D_2O. The buffer pH was adjusted to 7.3 using NaOD and D_2SO_4. 2 equivalents per Cu ion of 0.1 M freshly prepared dithionite solution in D_2O were added under Ar atmosphere to the Cu(II)-Aβ solution in a NMR sealed tube.

The ^{1}H NMR experiments were recorded on a Bruker Avance 500 spectrometer equipped with a 5 mm triple resonance inverse Z-gradient probe (TBI 1H, 31P, BB). The presaturation of the water signal was achieved with a zqpr sequence (Bruker). ^{1}H NMR experiments are performed at 298K.

HO• scavenging monitoring: test of equivalents

The experiment was performed following the procedure of a coumarin-3-carboxylic acid (CCA) assay previously described. CCA was used as a probe to detect HO• as it reacts with CCA to form the 7-hydroxycoumarin-3-carboxylic acid (7-OH-CCA), which is fluorescent at 450 nm upon excitation at 390 nm. The intensity of the fluorescence signal is proportional to the number of 7-OH-CCA molecules formed, which in turn is proportional to the HO• radicals released. Phosphate buffer was used, after treatment with Chelex,

as HEPES buffer can react with HO radicals. The fluorescence experiments were performed on a microplate reader FLUOstar OPTIMA (BMG Labtech). An automatic injector was used to add ascorbate (500 µM) at cycle 5 into the wells containing phosphate buffered solutions (50 mM, pH 7.4) solutions with CCA (500 µM), Cu^{2+} (50 µM) and the different tested peptides and mutants ($A\beta_{16}$; $A\beta_{16}$ double mutants: H6AH13A, H6AH14A; $A\beta_7$) at peptide:Cu ratios of 1.2, 1.5 and 2. Each one of the conditions was repeated at least 3 times to minimize errors.

The gradient for each condition was calculated for the first 360 seconds after the injection of ascorbate, and the plateau from an average of the fluorescence emission during the last 210 seconds. All the gradient/plateau values for the double mutants and $A\beta_7$ were normalized to those obtained for $A\beta_{16}$ to check there is no a significant difference between using 1.2 or > 1.2 equivalents of peptide.

Cu(I) coordination investigated by XANES spectroscopy

The N-terminal modification, or the addition or removal of 1 His residue on the Aβ sequence does not impact the Cu(I) binding mode, as shown in Figures S1 and S2. The XANES signatures of the Cu(I) complexes with modified peptides are similar to the XANES signature of Cu(I)-Aβ. As Cu(I) binds to 2 His residues, these results were expected.

When the Aβ peptide has only 1 His residue left on its sequence, the Cu(I) binding mode differs from the one of Cu(I)-Aβ. Figure S3 shows that $A\beta_7$-Cu(I) and (H6A-H13A)-Cu(I) complexes have similar Cu XANES signatures that are different from Cu(I)-$A\beta_{16}$ and Cu(I) in buffer signatures. The decrease of intensity of the pre-edge peak around 8980 eV indicates an increase of the number of ligands compared with Cu(I)-$A\beta_{16}$ (2 His residues as ligands). This has been previously addressed for Cu(I)-$A\beta_7$.[5]

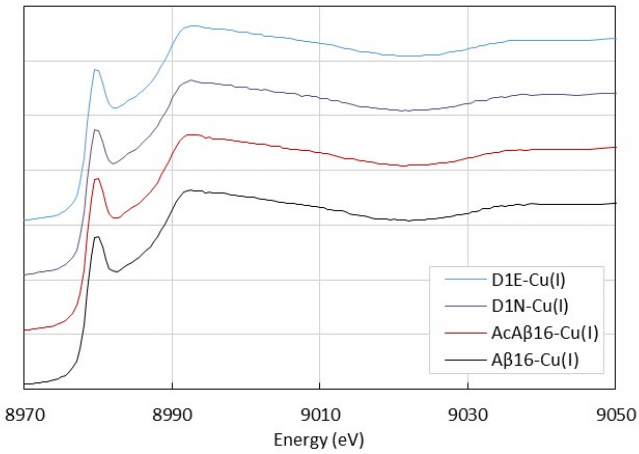

Figure S1: Cu XANES K-edge X-ray absorption spectra of $A\beta_{16}$-Cu(I) (black curve), $AcA\beta_{16}$-Cu(I) (red curve), D1N-Cu(I) (purple curve) and D1E-Cu(I) (blue curve) at pH 7.1.

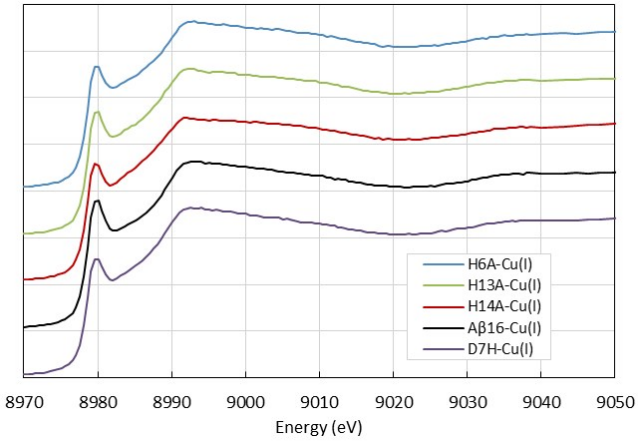

Figure S2: Cu XANES K-edge X-ray absorption spectra of $A\beta_{16}$-Cu(I) (black curve), H14A-Cu(I) (red curve), H13A-Cu(I) (green curve), D7H-Cu(I) (purple curve) and H6A-Cu(I) (blue curve) at pH 7.1.

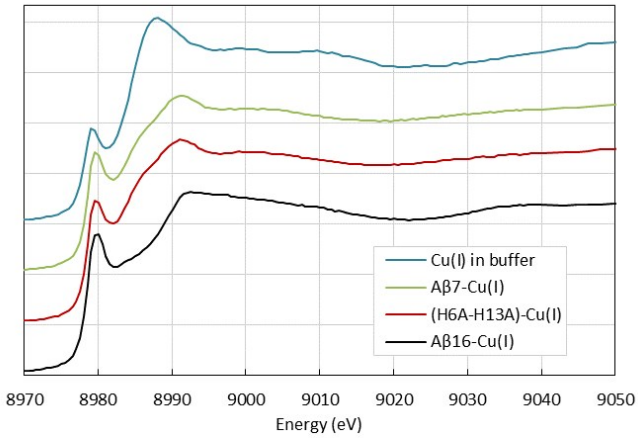

Figure S3: Cu XANES K-edge X-ray absorption spectra of $A\beta_{16}$-Cu(I) (black curve), (H6A-H13A)-Cu(I) (red curve), $A\beta_{7}$-Cu(I) (green curve) and Cu(I) in buffer (blue curve) at pH 7.1.

Cu(II) coordination investigated by EPR spectroscopy

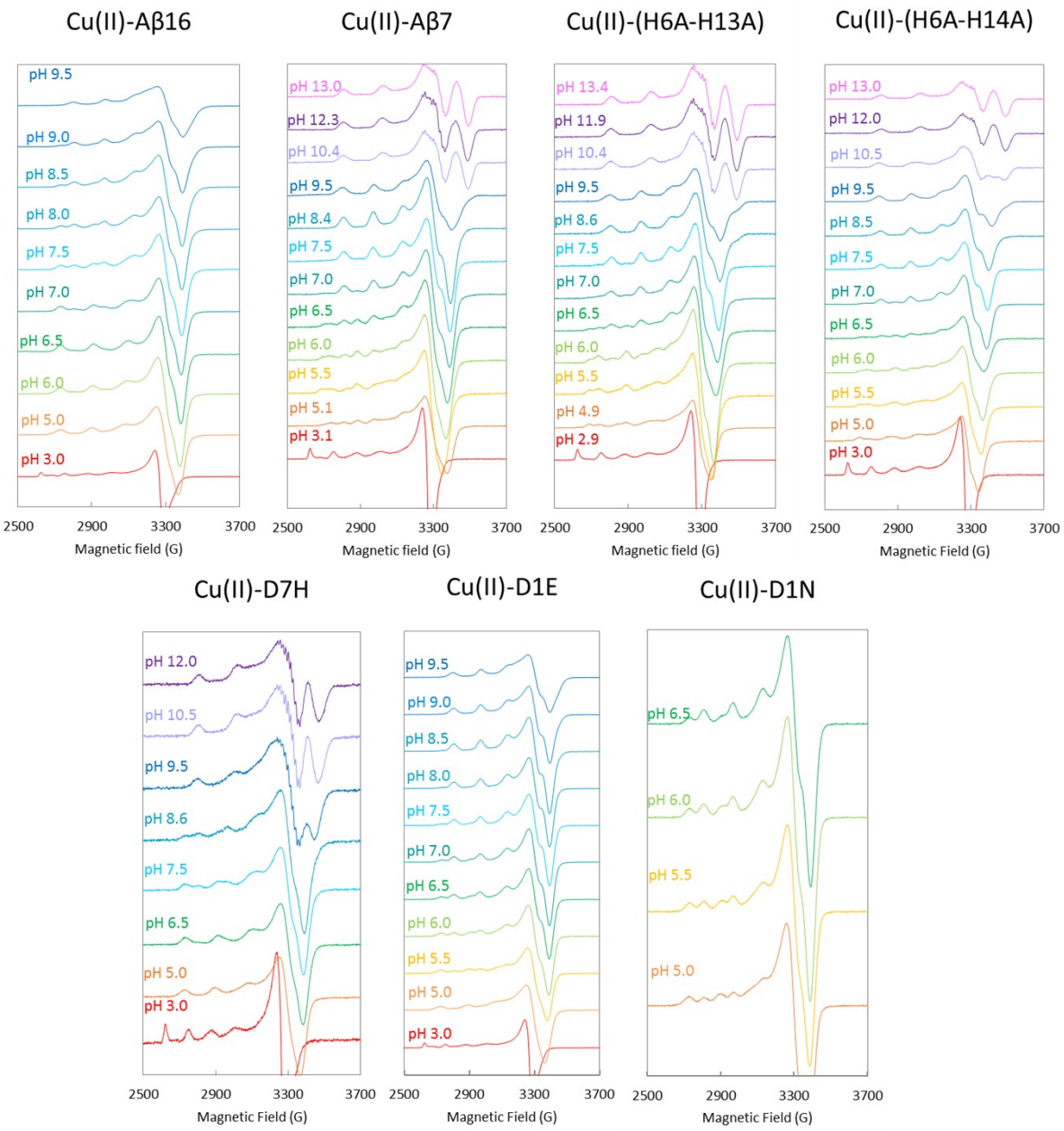

Figure S4 : EPR spectra of ^{65}Cu(II) coordinated to $A\beta_{16}$, $A\beta_7$, H6A-H13A, H6A-H14A, D7H, D1E or D1N at different pH. Aqueous solution of ^{65}Cu(II) (0.45 mM), peptide (0.5 mM) with 10 % of glycerol.

The EPR parameters shown in Table S1 have been calculated from the EPR spectra of Figure S4 for each ^{65}Cu(II)-peptide complex. The pKa(I/II) value and the $g_{//}$ and $\mathcal{A}_{//}$ values of components I et II of Cu(II)-$A\beta_{16}$ obtained are similar to the literature.[6] The same results are obtained with D7H, meaning that the addition of one His residue in the sequence does not have any consequence on the coordination mode of Cu(II).

For the $A\beta_7$, H6A-H13 and H6A-H14A peptides which have only one His residue, the Cu(II) ion is bound to them as a component II, as shown by the $g_{//}$ and $\mathcal{A}_{//}$ values close to the Cu-$A\beta_{16}$ component II. It was expected as only one His residue is involved in the coordination sphere of the component II.

EPR parameters obtained for D1N are also in line with the literature [7] and are very similar to those obtained with D1E. Thus, as well as D1N mutation, the mutation of Asp1 by a Glu residue only leads to a decrease of the pKa(I/II) value from 7.8 to 6.0.

Table S1: EPR parameters of components I and II of $^{65}Cu(II)$-peptides complexes along with the pKa values of components I and II and their equatorial binding mode.

Peptide	Component	$g_{//}$	$\mathcal{A}_{//}$ (10^{-4} cm^{-1})	pKa (I/II)	Equatorial binding mode
$A\beta_{16}$	I	2.27	181	7.8	NH_2 (D1), CO (D1-A2), N_{im} (H6), N_{im} (H13 or H14)
	II	2.23	158		NH_2 (D1), N^- (D1-A2), CO (A2-E3), N_{im}
$A\beta_7$	II	2.22	158	Major species from pH 6	NH_2 (D1), N^- (D1-A2), CO (A2-E3), N_{im}
H6A-H13A	II	2.22	162		
H6A-H14A	II	2.23	164		
D7H	I	2.27	181	7.8	NH_2 (D1), CO (D1-A2), N_{im} (H6), N_{im}
	II	2.24	151		NH_2 (D1), N^- (D1-A2), CO (A2-E3), N_{im}
D1E	I	2.28	184	6.0	NH_2 (E1), CO (E1-A2), N_{im} (H6), N_{im} (H13 or H14)
	II	2.23	163		NH_2 (E1), N- (E1-A2), CO (A2-E3), N_{im}
D1N	I	2.28	181	6.0	NH_2 (N1), CO (N1-A2), N_{im} (H6), N_{im} (H13 or H14)
	II	2.23	157		NH_2 (N1), N- (N1-A2), CO (A2-E3), N_{im}

Parallel spin Hamiltonian parameters ($g_{//}$ and $\mathcal{A}_{//}$) were obtained directly from the experimental spectra and were calculated from the second and the third hyperfine lines in order to remove second-order effects. $\mathcal{A}_{//}$ parameters are calculated for ^{63}Cu isotope for comparison with the litterature, by using the ratio $g_n(^{65}Cu)/\ g_n(^{63}Cu) = 1.07$ for comparison with the litterature. pKa values are estimated from EPR spectra with an uncertainty of ±0.3 pH unit.

^{1}H NMR of 1-His peptides with Cu(I)

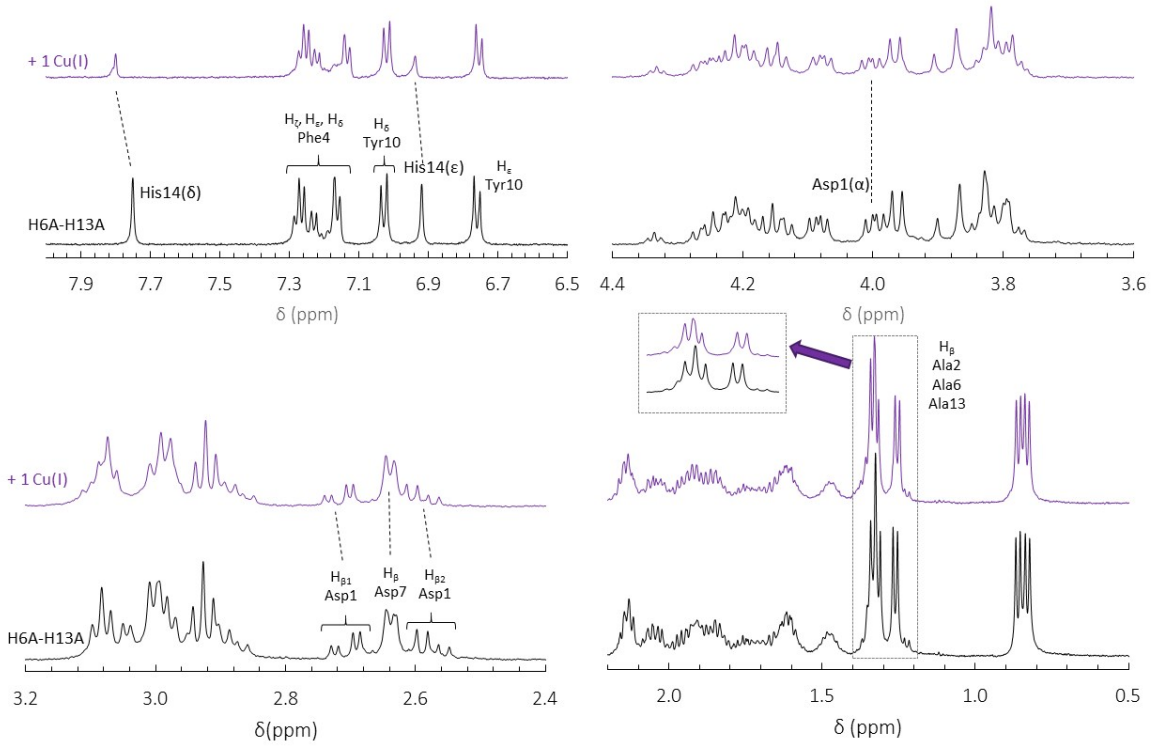

Figure S5: ^{1}H NMR spectra of H6A-H13A (black curve) and H6A-H13A with 1 equivalent of Cu(I) (purple curve) at pH 7.3. The chemical shifts of protons observed with the addition of Cu(I) are indicated with dotted lines. All chemical shifts were referenced at 0.00 ppm relative to internal TSP.

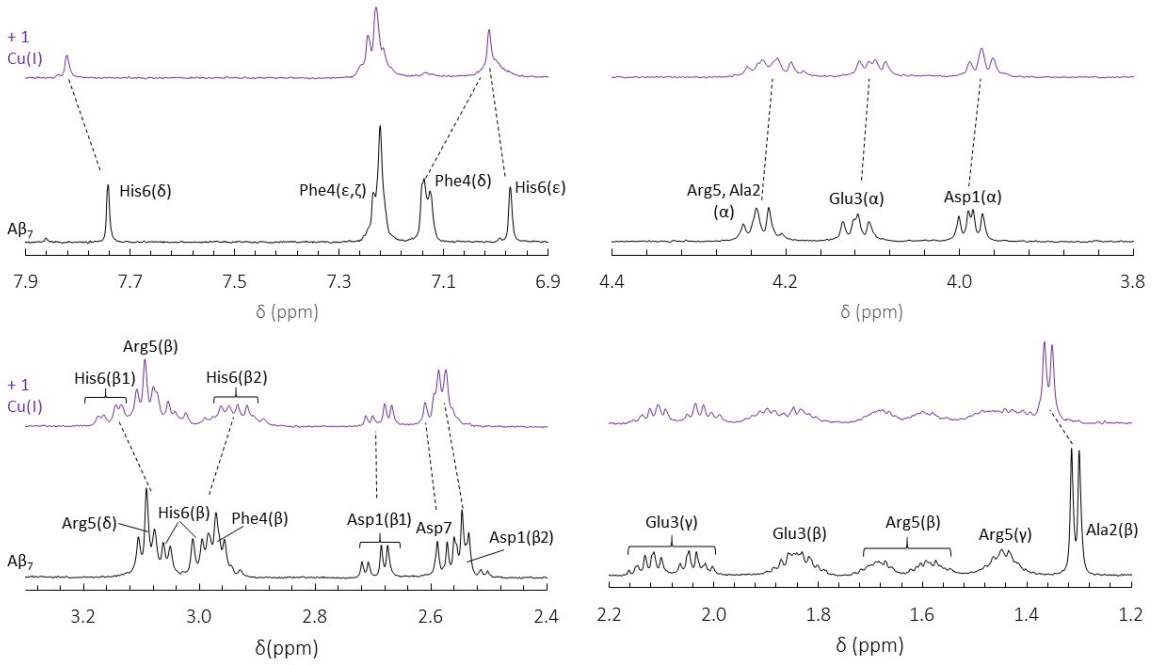

Figure S6: ^{1}H NMR spectra of Aβ$_7$ (black curve) and Aβ$_7$ with 1 equivalent of Cu(I) (purple curve) at pH 7.3. The chemical shifts of protons observed with the addition of Cu(I) are indicated with dotted lines. All chemical shifts were referenced at 0.00 ppm relative to internal TSP.

$A\beta_7$: a special case

The Cu(I) metal ion binding with amino acid residues modifies the electron density of the protons, and results in a chemical shift of the protons close to the Cu(I). As an example, in Figure S6, the H_δ, H_ε and H_β protons of His6, present at about 7.75, 6.97 and 3.04 ppm, are strongly shifted. Thus, His6 residue of $A\beta_7$ is involved in Cu(I) binding.

Both Hα (around 4.23 ppm) and H_β (around 1.30 ppm) protons of Ala2 are also strongly shifted with the addition of Cu(I). As the chemical shift of Ala protons is very sensitive to the chemical environment, and since Ala2 residue cannot bind metal ions, it is expected that an amino acid residue close to Ala2 is bound to Cu(I) ion. Except H_α of Glu3 which is shifted (around 4.12 ppm), the other protons are not really impacted by the addition of Cu(I). Thus, it is unlikely that Glu3 is a Cu(I) ligand, and neither Arg5 residue as its protons (at 1.44, 1.60, 1.68 and 3.10 ppm) are not shifted in the presence of Cu(I). For Asp1, H_α and $H_{\beta2}$ are also impacted by Cu(I) addition (3.98 and 2.56 ppm). Asp1 has a terminal amine group, Cu(I) is probably coordinated to the N-terminal NH_2 of Asp1. This is in line with the higher affinity of Cu(I) for nitrogen atom than for oxygen atom. However, the $H_{\beta1}$ peak (around 2.68 ppm) being not shifted, the carboxylate group of Asp1 seems to not be involved in the coordination sphere of Cu(I). These results are supported by the ^1H NMR spectra of $A\beta_{16}$ in which the Asp1 and Ala2 protons are not shifted in the presence of Cu(I) (See Figure 4).

The carboxylate group of Asp7 in $A\beta_7$ is also proposed to be involved in Cu(I) coordination. The two H_β protons, whose chemical shift is close to the one of Asp1 $H_{\beta2}$ proton (around 2.56 ppm), are also strongly shifted. For Phe4, although its H_ε and H_ζ protons keep the same chemical shift in the presence of Cu(I) (at 7.22 ppm), H_δ (7.13 ppm) and H_β (2.97 ppm) peaks shift and get wider with the addition of Cu(I). This was also observed with $A\beta_{16}$ (Figure 4) and is probably linked to the reorganization of the peptide 3D structure due to the coordination of Aβ with the Cu(I).

^1H NMR experiments on $A\beta_7$ with Cu(I) confirm the increase of the number of ligands for Cu(I) in the $A\beta_7$ peptide that was previously shown by Cu(I) K-edge XANES.[5] The proposed ligands for Cu(I)-$A\beta_7$ coordination are the terminal NH_2 of Asp1, a N atom of the imidazole ring of His6 and the carboxylate group of Asp7. Thus, unlike H6A-H13A and H6A-H14A, the closeness of His6 (a ligand of Cu(I)) with Asp7 leads to the coordination of the carboxylate group of Asp7 instead of the one of Asp1 in the case of $A\beta_7$.

Metal-catalyzed ROS production by Cu ion with modified Aβ peptides

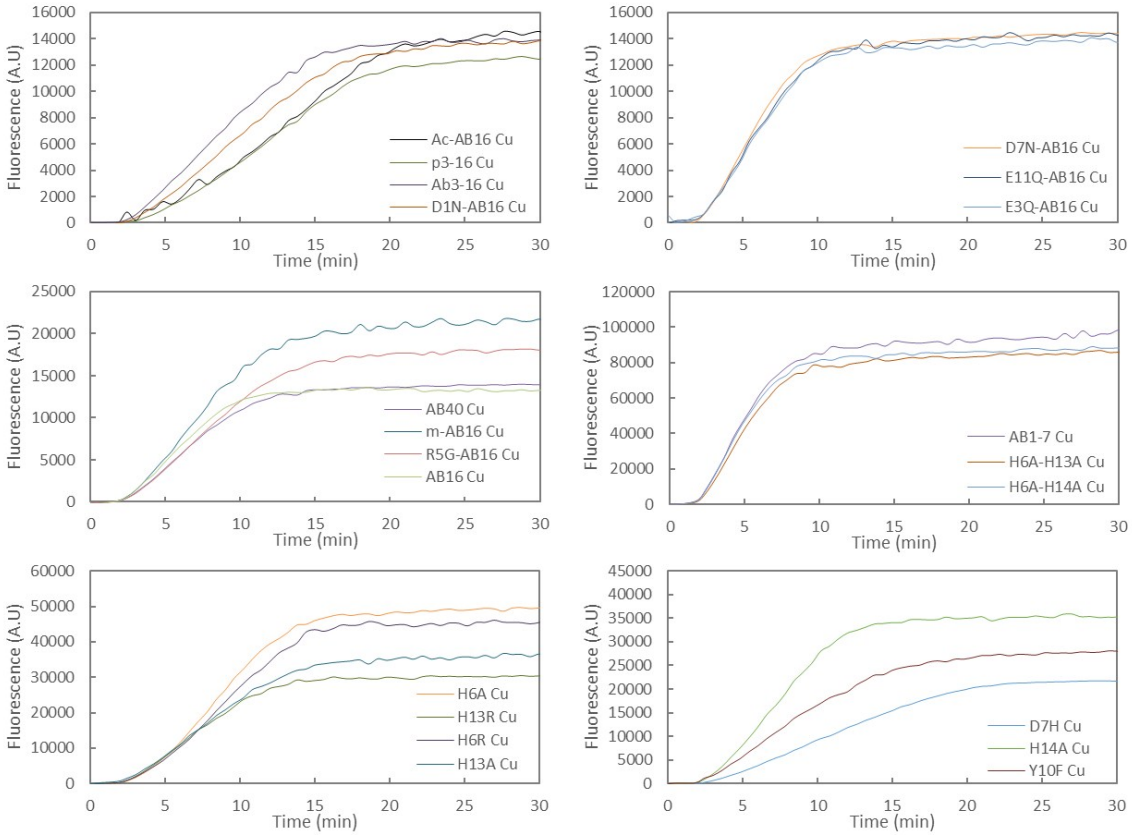

Figure S7: Fluorescence curves of ROS production. Fluorescence of the 7-OH-CCA ($\lambda_{ex\ c}$= 395 nm, λ_{em} = 452 nm) as a function of the time, showing the scavenging kinetics of HO• produced by Cu^{2+} (50µM), ascorbate (500µM) and peptide (60µM) in phosphate-buffered solution (pH 7.4, 50 mM) with CCA (500 µM). The curves of the 22 peptides with copper are represented.

Gradient and fluorescence at the plateau values inform on the rate of 7-OH-CCA formation and on the quantity of 7-OH-CCA formed, respectively. However, they cannot be directly linked to the rate and quantity of HO• produced by the Cu-Aβ system. Indeed, the total amount of ROS produced by Cu-Aβ in the presence of ascorbate only depends on ascorbate and dioxygen concentrations, the process being catalytic.
Thus, the same ascorbate concentration should lead to the same total fluorescence at the plateau (after HO• has been trapped by CCA). But this is not the case, since for His-Ala single mutants and D7H, the value of fluorescence at the plateau is stronger and weaker than the one obtained for $Aβ_{16}$, respectively (Figure 7b, main text). As shown previously, Aβ is also a target for the hydroxyl radicals and the coordination of copper influences the HO• release.[8] The analysis of the trend obtained for the His mutants clearly shows that higher the number of His, lower the value at the plateau. This is confirmed by High-Resolution Mass Spectrometry (LC-HRMS) experiments showing that ratio of N-terminal oxidation vs. the other oxidations decreases when increasing the number of His in the peptide sequence (Figure S7, Tables S2 and S3). Thus, the total amount of HO• released by the Cu-Aβ system is dependent on the peptide nature (number of potential targets for HO• and spatial arrangement of the peptide when coordinated to the copper ion). This has also an influence on the gradient-values obtained in the fluorescence curves, meaning on the HO• exiting the system per time unit. Thus, the relative gradient to plateau ratio was calculated in order to evaluate the intrinsic rate of HO• release (i.e. independent of the HO• by the peptide) (Figure 7c, main text).

ANOVA analysis from CCA assay:

Data from slope
One Way ANOVA
Data Table: Slope data

Factor A: 23 Groups
D7H, Ac-Ab16, p3-16, Ab3-16, D1E, D1N, Ab16, Ab40, E3Q, Y10F, D7N, R5G, E11Q, H6A, H6R, H13A, H13R, m-Ab16, H14A, H6AH13A, H6A-H14A, Ab1-7, Cu

Analysis of Variance Results

Source	DF	SS	MS	F	P
Total	251	7347.3493	29.272308		
A	22	7066.4303	321.20138	261.83744	< .0001
Error	229	280.91901	1.2267206		

Data from plateau
One Way ANOVA
Data Table: Plateau data
Factor A: 23 Groups
D7H, Ac-Ab16, p3-16, Ab3-16, D1E, D1N, Ab16, Ab40, E3Q, Y10F, D7N, R5G, E11Q, H6A, H6R, H13A, H13R, m-Ab16,
H14A, H6AH13A, H6A-H14A, Ab1-7, Cu

Analysis of Variance Results

Source	DF	SS	MS	F	P
Total	251	793.52498	3.1614541		
A	22	781.61488	35.527949	683.10898	< .0001
Error	229	11.910106	0.052009196		

Data from slope/plateau
One Way ANOVA
Data Table: Slope-plateau data
Factor A: 23 Groups
D7H, Ac-Ab16, p3-16, Ab3-16, D1E, D1N, Ab16, Ab40, E3Q, Y10F, D7N, R5G, E11Q, H6A, H6R, H13A, H13R, m-Ab16,
H14A, H6AH13A, H6A-H14A, Ab1-7, Cu

Analysis of Variance Results

Source	DF	SS	MS	F	P
Total	251	145.42272	0.57937338		
A	22	133.06051	6.048205	112.03816	< .0001
Error	229	12.362207	0.053983439		

Detection of oxidation on native and modified Aβ peptides after metal-catalyzed ROS production by High-Resolution Mass Spectrometry

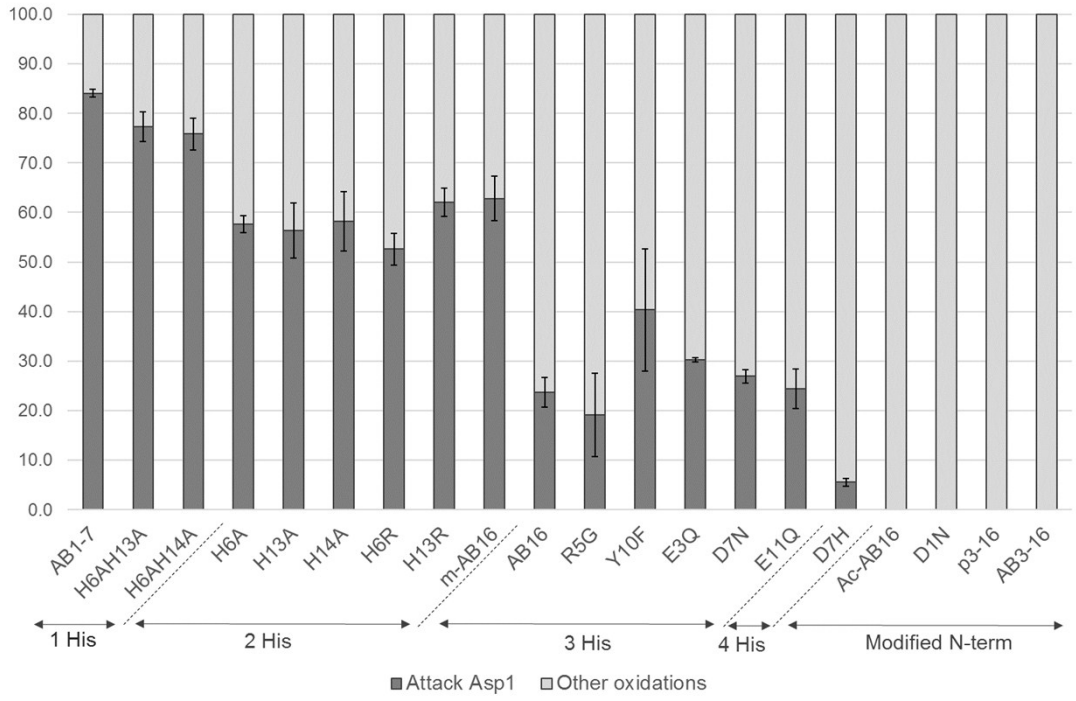

Figure S8: Relative proportions (in percent, + standard deviation) of the specific oxidations on Asp1 and the non-specific oxidations detected for the native and modified Aβ peptides under focus, after oxidation in the presence of copper and ascorbate. Operating conditions are similar as for fluorescence study. Specific oxidations on Asp1 are indicated in dark grey while the other oxidations are in light grey. The nature of the oxidations are listed in Table S2 and the different proportions of each oxidation are indicated in Table S3.

Table S2: abbreviation used for the oxidation products of Aβ, as previously identified.[8]

Specific of Asp1	**dd**	Decarboxylation/deamination of Asp1, leading to a mass loss of 45 Da
	ox	Oxidative fragmentation of Asp1, leading to a mass loss of 89 Da
Not specific	**+14**	Formal addition of one atomic oxygen, followed by a dehydrogenation
	+16	Formal addition of one atomic oxygen

Table S3: Relative proportions (in percent, + standard deviation) of the oxidation products detected for the native and modified Aβ peptides under focus, after oxidation in the presence of copper and ascorbate. Operating conditions are similar as for fluorescence study.

Peptide	Non ox		dd*		ox*		+16/+32		+14/+28	
AB1-7	4.1	*(2.4)*	15.7	*(1.2)*	64.9	*(1.8)*	10.8	*(0.4)*	4.5	*(0.6)*
H6AH13A	2.3	*(0.6)*	13.2	*(0.8)*	62.4	*(3.1)*	18.9	*(2.3)*	3.2	*(0.5)*
H6AH14A	0.9	*(0.3)*	12.0	*(0.8)*	63.2	*(3.3)*	20.7	*(2.7)*	3.3	*(0.5)*
H6A	0.5	*(0.1)*	11.3	*(1.5)*	46.1	*(2.9)*	27.8	*(2.1)*	14.4	*(0.7)*
H13A	4.7	*(4.2)*	18.0	*(1.8)*	35.9	*(8.9)*	28.5	*(5.3)*	12.8	*(1.9)*
H14A	1.9	*(1.7)*	14.7	*(2.7)*	42.5	*(9.4)*	27.4	*(6.5)*	13.5	*(1.5)*
H6R	0.4	*(0.4)*	15.2	*(4.4)*	37.2	*(2.3)*	35.9	*(2.3)*	11.3	*(5.3)*
H13R	3.5	*(2)*	15.6	*(3.1)*	44.3	*(2.7)*	26.1	*(2.3)*	10.5	*(5.3)*
m-AB16	11.3	*(3.3)*	16.4	*(8.2)*	39.4	*(3.7)*	24.6	*(3.4)*	8.3	*(0.8)*
AB16	2.9	*(3.4)*	3.5	*(2)*	19.5	*(3.8)*	44.8	*(4.4)*	29.2	*(7.9)*
R5G	23.4	*(14.7)*	1.7	*(1.1)*	14.0	*(8.2)*	48.3	*(1.3)*	12.6	*(5)*
Y10F	0.3	*(0.3)*	17.3	*(8.6)*	23.0	*(4)*	30.5	*(9)*	29.0	*(3.3)*
E3Q	5.5	*(3.2)*	5.1	*(0.6)*	23.5	*(1.2)*	46.4	*(3.5)*	19.5	*(2.6)*
D7N	4.9	*(3)*	4.7	*(1.2)*	20.9	*(0.8)*	50.9	*(2.4)*	18.6	*(1.8)*
E11Q	6.2	*(3.5)*	3.3	*(1.2)*	19.6	*(2.1)*	54.2	*(5.7)*	16.8	*(2.4)*
D7H	0.7	*(0.4)*	0.2	*(0.4)*	4.7	*(0.2)*	46.0	*(18)*	48.4	*(18.4)*
Ac-AB16	6.4	*(2.5)*	*nd*		*nd*		68.0	*(3.9)*	25.6	*(1.4)*
D1N	4.6	*(2.2)*	*nd*		*nd*		66.6	*(2.1)*	28.8	*(2.9)*
p3-16	2.2	*(2.1)*	*nd*		*nd*		66.6	*(2.5)*	31.2	*(3.5)*
AB3-16	0.4	*(0.3)*	*nd*		*nd*		57.2	*(5)*	42.4	*(5)*

nd = not detected

** includes [dd, dd+14 and dd+16] or [ox, ox+14 and ox+16], i.e. primary and secondary oxidation products (re-oxidation of a primary oxidized Aβ).*

HO• scavenging monitoring: test of equivalents

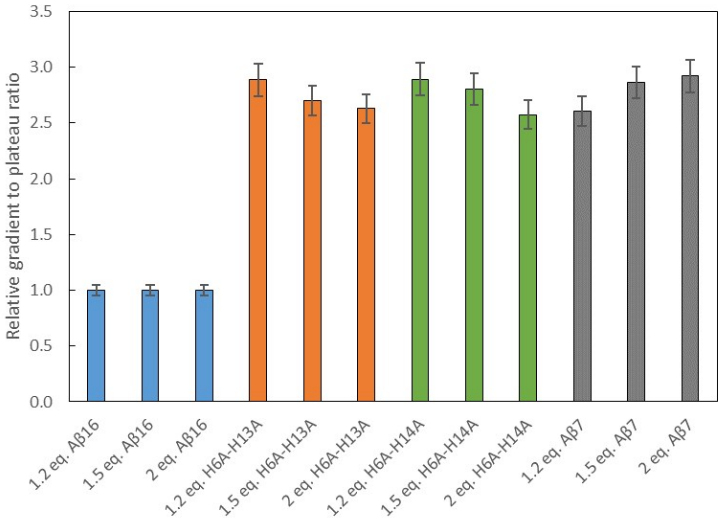

Figure S9: HO• scavenging by CCA. Gradient to plateau ratio of 7-OH-CCA fluorescence resulting from oxidation of CCA 500 µM in the presence of ascorbate 500 µM, Cu(II) 50 µM and native or modified Aβ peptides (1.2, 1.5 or 2 equivalents for 1 Cu). Phosphate-buffered (50 mM) solutions at pH 7.4.

For each peptide, similar relative HO• production rates are obtained with 1.2, 1.5 and 2 equivalents of peptide by Cu ion. The results show that the higher HO• production rate obtained with the 1-His peptides ($A\beta_7$, H6A-H13A and H6A-H14A) is not due to a contribution of free copper.

Ascorbate consumption by Cu ion with modified Aβ peptides at different pH.

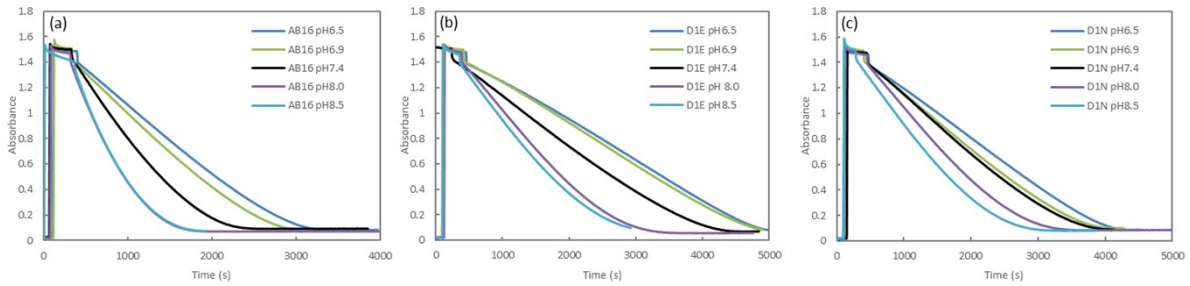

Figure S10: UV-Visible curves of ascorbate oxidation. Absorbance at 265 nm of ascorbate (100 µM) as a function of the time by Cu (10 µM) bound to $A\beta_{16}$ (a), D1E-Aβ16 (b) or D1N-Aβ16 (c) (20 µM) in HEPES buffered solution (pH 6.5, 7.0, or 7.4) or POPSO buffered solution (pH 8.0 or 8.5).

Determination of the pKa value of the NH_2(Asp1) of $A\beta_{16}$ in the presence of Cu(I) by ^1H NMR

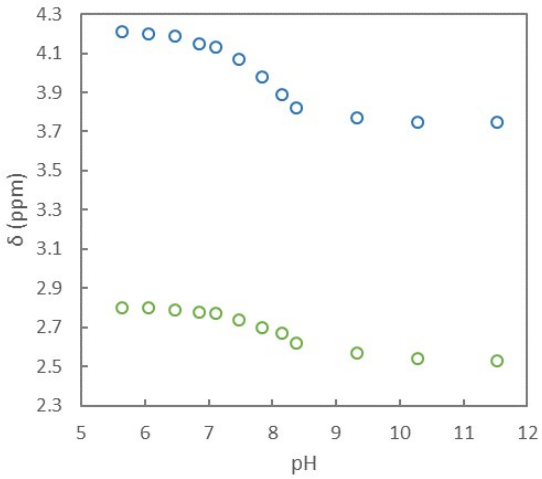

Figure S11: Chemical shifts of the H_α and $H_{\beta1}$ of the Asp1 residue of $A\beta_{16}$ as a function of pH, in the presence of Cu(I). **pKa value: 7.8.**

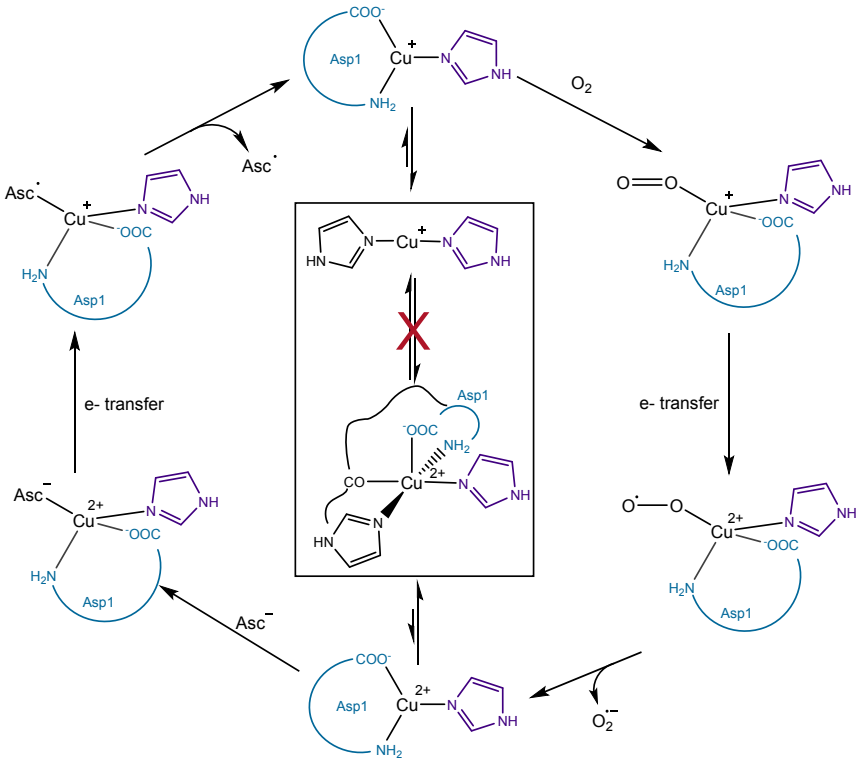

Figure S12. Schematic representation of the proposed mechanism of electron transfer between Cu(II)-Aβ and ascorbate (Asc-) and between Cu(I)-Aβ and O_2 leading to the formation of $O_2^{\bullet-}$. Cu binding modes in the RS (rectangle) and Cu binding modes of the species in the CIBS during the production of $O_2^{\bullet-}$. Asc$^\bullet$ represents ascorbyl radical.

References

1. O. Proux, X. Biquard, E. Lahera, J. Menthonnex, A. Prat, O. Ulrich, Y. Soldo, P. Trévisson, G. Kapoujyan and G. Perroux, *Phys. Scr.*, 2005, **2005**, 970.
2. O. Proux, V. Nassif, A. Prat, O. Ulrich, E. Lahera, X. Biquard, J.-J. Menthonnex and J.-L. Hazemann, *Journal of synchrotron radiation*, 2006, **13**, 59-68.
3. R. Delgado, J. F. Da Silva, M. Amorim, M. Cabral, S. Chaves and J. Costa, *Anal. Chim. Acta*, 1991, **245**, 271-282.
4. A. Krężel and W. Bal, *J. Inorg. Biochem.*, 2004, **98**, 161-166.
5. C. Cheignon, P. Faller, D. Testemale, C. Hureau and F. Collin, *Metallomics*, 2016, **8**, 1081-1089.
6. C. Hureau, *Coord. Chem. Rev.*, 2012, **256**, 2164-2174.
7. B. Alies, H. Eury, C. Bijani, L. Rechignat, P. Faller and C. Hureau, *Inorg. Chem.*, 2011, **50**, 11192-11201.
8. L.-E. Cassagnes, V. Hervé, F. Nepveu, C. Hureau, P. Faller and F. Collin, *Angew. Chem. Int. Ed.*, 2013, **52**, 11110-11113.